

# Quantifying long-range correlations in complex networks beyond nearest neighbors

D. RYBSKI<sup>1(a)</sup>, H. D. ROZENFELD<sup>2,3</sup> and J. P. KROPP<sup>1</sup>

<sup>1</sup> *Potsdam Institute for Climate Impact Research - 14412 Potsdam, Germany, EU*

<sup>2</sup> *Levich Institute, City College of New York - New York, NY 10031, USA*

<sup>3</sup> *Division of Natural Sciences, College of Mount Saint Vincent - Riverdale, NY 10471, USA*

received 20 November 2009; accepted in final form 9 April 2010  
published online 13 May 2010

PACS 89.75.Fb – Structures and organization in complex systems  
PACS 05.40.-a – Fluctuation phenomena, random processes, noise, and Brownian motion  
PACS 05.45.Df – Fractals

**Abstract** – We propose a fluctuation analysis to quantify spatial correlations in complex networks. The approach considers the sequences of degrees along shortest paths in the networks and quantifies the fluctuations in analogy to time series. In this work, the Barabasi-Albert (BA) model, the Cayley tree at the percolation transition, a fractal network model, and examples of real-world networks are studied. While the fluctuation functions for the BA model show exponential decay, in the case of the Cayley tree and the fractal network model the fluctuation functions display a power law behavior. The fractal network model comprises long-range anticorrelations. The results suggest that the fluctuation exponent provides complementary information to the fractal dimension.

Copyright © EPLA, 2010

**Introduction.** – Networks, consisting of simple elements, its nodes and links, can display complex properties, such as a broad degree distribution, clustering, modularity, and many others. This work focuses on the correlation between node degrees —the number of links attached to a node. Degree correlations, measuring the likelihood that nodes of a given degree are connected, help to explain important features of complex networks that are beyond the degree distribution or clustering. For instance, it has been found that many networks, such as the coauthorship, film actor (IMDb —Internet Movie Database), and company directors networks display assortative mixing between degrees, indicating that nodes of like degree tend to be connected. On the other hand, the Internet (autonomous system), the WWW, and some biological networks, exhibit disassortative mixing, where there is a high tendency for high-degree nodes (hubs) to be connected to low-degree nodes [1,2].

Different ways to quantify degree correlations are defined and used in the literature. One measure is the Pearson correlation coefficient of all linked pairs of nodes [1] which derives from the probability distribution  $p(k_1, k_2)$  that two nodes of degree  $k_1$  and  $k_2$  are connected through a link [3,4]. Another measure of

degree correlations is the average degree of neighbors of a degree- $k$  node [3]. This measure may also be obtained as a particular case of the matrix  $p(k_1, k_2)$ , and classifies networks into assortative (disassortative) when this quantity increases (decreases) with  $k$ . Furthermore, it has been shown that disassortativity reflected in  $p(k_1, k_2)$  is a tightly related property to fractality in complex networks [5,6].

The different measures of degree correlations consider only correlations between nearest-neighbor nodes, *i.e.* only correlations between the degrees of nodes at distance 1, but not further. Because of this limitation, these measures fail to capture much of the rich topological information of the network. In this work we introduce an approach that extends the idea of degree correlations to larger distances. An immediate extension of previous methods could consist on simply considering the correlation coefficient from nearest neighbors to the second, the third,  $\dots$   $d$ -th neighbors. However, in complex networks the direct calculation of such a function is not feasible. Here we introduce a *fluctuation analysis* that overcomes this issue. We study the fluctuations of the degree along shortest paths between two nodes and consider the distance between nodes analogous to time in time-series analysis. Our approach can be adapted to study many topological and dynamical correlation properties in networks, such as node activity, node

<sup>(a)</sup>E-mail: ca-dr@rybski.de

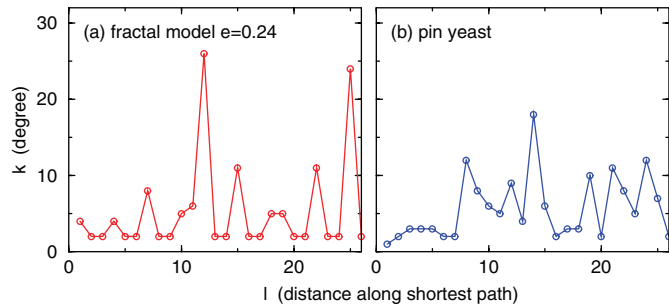


Fig. 1: (Colour on-line) Examples of degree sequences along shortest paths. For arbitrary shortest paths we plot the degree of the nodes *vs.* the distance for (a) the fractal network model with  $e = 0.24$  ( $\alpha_k \approx -0.65$ ) and (b) the pin yeast network ( $\alpha_k \approx -0.53$ ).

weights, time of node addition, etc. In this work we introduce the formalism and focus on degree correlations, leaving other properties for further investigation.

**Fluctuation analysis.** – In order to quantify long-range degree (anti)correlations at distances larger than nearest neighbors, we propose a fluctuation analysis. The method consists of the following steps:

- 1) Find the shortest path between all pairs of nodes in the network (if the shortest path between a pair of nodes is not unique, then we consider an arbitrary one), see fig. 1.
- 2) Consider all shortest paths of length  $d$  and calculate the average  $K_d = \langle k_l \rangle$  of the sequence  $(k_l)$  of node degrees along each of these paths of length  $d$ , where  $1 \leq l \leq (d+1)$ .
- 3) Repeat the previous step for all possible values of  $d$  in the network.
- 4) Calculate the fluctuation function  $F(d) = \sigma(K_d|d)$ , which is the conditional standard deviation of the  $K_d$  at distance  $d$ , *i.e.* the standard deviation of the averages  $K_d$  for those paths of length  $d$ .

The fluctuation function describes the correlations of node degrees along shortest paths [7–10]. When an uncorrelated time series is partitioned into segments of size  $s$ , the standard deviation of the segments averages decays as  $\sigma \sim s^{-1/2}$ .

Because the overall distance between nodes in a network is short (compared to the time span of time series), we do not partition the degree sequences into segments. Instead, we consider all shortest path of any length  $d$ . Thus, if the covariance,  $C(d)$ , between the degree of nodes at distance  $d$  scales as  $C(d) \sim \langle (k_i - \langle k \rangle)(k_j - \langle k \rangle) | d \rangle \sim d^{-\gamma}$ , where  $\langle k \rangle$  is the average degree of the network, then for the fluctuation function we expect

$$F(d) \sim d^{\alpha_k}, \quad (1)$$

where  $\alpha_k = -\gamma/2$ . Notice that because the average (calculated in step 2) involves a division by  $d$ , the degree fluctuation exponent  $\alpha_k$  differs by 1 from the usual Hurst-like exponent  $\alpha$  [11] of time series analysis:  $\alpha_k = \alpha - 1$ . For asymptotical  $\alpha_k = -1/2$  ( $\alpha = 1/2$ ) the degrees are uncorrelated.

Starting from the average degree along a shortest path,  $K_d = \frac{1}{d+1} \sum_{j=1}^{d+1} k_j$ , we can express the variance as follows [11]:

$$\sigma^2(K_d|d) = \langle (K_d - \langle K_d \rangle)^2 \rangle, \quad (2)$$

where  $\langle K_d \rangle$  is the average over all values of  $K_d$ . Therefore, assuming  $\langle K_d \rangle \simeq \langle k \rangle$ , we find

$$\begin{aligned} \sigma^2(K_d|d) &\simeq \frac{1}{(d+1)^2} \left\langle \sum_{j=1}^{d+1} (k_j - \langle k \rangle)^2 \right\rangle \\ &+ \frac{1}{(d+1)^2} \left\langle \sum_{\substack{j,l \leq d+1 \\ j \neq l}} [(k_j - \langle k \rangle)(k_l - \langle k \rangle)] \right\rangle \\ &= \frac{1}{(d+1)} \langle (k_j - \langle k \rangle)^2 \rangle \\ &+ \frac{1}{(d+1)^2} \sum_{\substack{j,l \leq d+1 \\ j \neq l}} C(|j-l|) \\ &= \frac{1}{(d+1)} \langle (k_j - \langle k \rangle)^2 \rangle \\ &+ \frac{2}{(d+1)^2} \sum_{j=1}^d (d+1-j)C(j). \end{aligned}$$

In the case of (positive) long-range correlations with correlation exponent  $\gamma$ , the second term dominates. In the limit of large  $d$  we can integrate the sum, leading to the approximation

$$\begin{aligned} \sigma^2(K_d|d) &\sim \frac{2}{(d+1)^2} d^{2-\gamma}, \\ \sigma(K_d|d) &\sim d^{-\gamma/2}. \end{aligned} \quad (3)$$

With eq. (1) and  $F(d) = \sigma(K_d|d)$  we obtain

$$\alpha_k = -\gamma/2. \quad (4)$$

While positive long-range correlations are characterized by fluctuation exponents  $-1/2 < \alpha_k < 0$  [11], negative long-range correlations (long-range anticorrelations) are characterized by fluctuation exponents  $-1 < \alpha_k < -1/2$  [12–14]. For the former, the covariance scales as  $C(d) \sim d^{-\gamma}$  and for the latter we assume  $C(d) \sim -(d^{-\gamma})$ .

### Results. –

*Barabasi-Albert model.* First we investigate the Barabasi-Albert (BA) model which is based on preferential attachment and has been introduced to generate scale-free networks [15] with power law degree distribution  $p(k) \sim k^{-3}$ . The BA model consists of subsequently

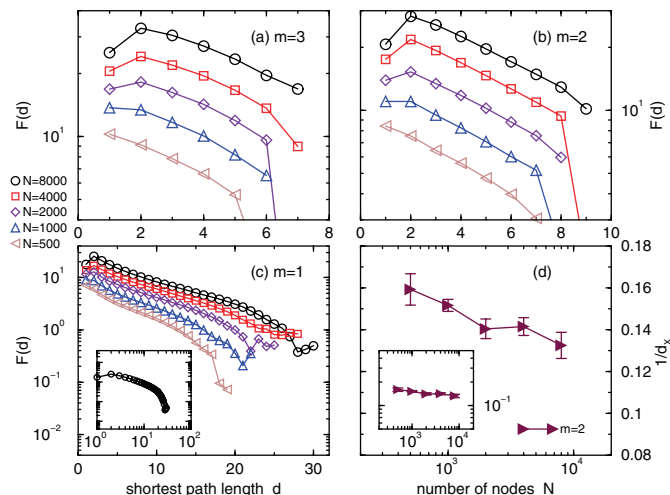


Fig. 2: (Colour on-line) Degree fluctuation functions for the BA model. The fluctuation functions,  $F(d)$ , are plotted against the length of the shortest paths  $d$ , for (a)  $m = 3$ , (b)  $m = 2$ , and (c)  $m = 1$ . The panels (a-c) show  $F(d)$  for networks consisting of 500, 1000, 2000, 4000, and 8000 nodes (from bottom to top). Panel (d) shows for  $m = 2$  the slopes of exponential fits applied to  $F(d)$  as a function of the network sizes. The insets in (c) and (d) are the same as the corresponding panels but in double-logarithmic representation (inset (c) only  $N = 8000$ ). For each set 100 configurations have been averaged.

adding nodes to the network and linking them to  $m$  already existing nodes which are randomly chosen with a probability proportional to their degree. In this model, the parameter  $m$  denotes the number of links attached to a new node. Therefore, the larger the  $m$ , the more cycles are generated in the network. In addition, when  $m$  is large the overall diameter of the network—the longest shortest path between all pairs of nodes—decreases due to the increased number of paths between any pair of nodes.

In order to analyze the correlations in BA model networks we generate 100 configurations, apply the fluctuation analysis, and calculate the degree fluctuation function  $F(d)$  among all configurations. Figure 2 shows the obtained  $F(d)$  for  $m = 1, 2, 3$  and different network sizes  $N = 500, 1000, \dots, 8000$  nodes in semi-logarithmic scale. The fluctuation function approximately decays exponentially according to  $F(d) \sim e^{-d/d_x}$ . In the case of  $m = 2$  (fig. 2b) straight lines between  $d = 2$  and  $d = 8$  are found, almost parallel for the different sizes.

The dependence on the network size is shown in fig. 2d where for  $m = 2$  the slope  $1/d_x$  is plotted vs. the number of nodes  $N$ . In this case, the slope varies between  $1/d_x \approx 0.16$  for the small networks and  $1/d_x \approx 0.13$  for the larger ones. Further investigations are needed to clarify if the slope reaches an asymptotic value. The BA model has been shown to be almost uncorrelated [1,3] and from an analogy with times series analysis, one would expect that the fluctuation function decreases according to eq. (1) with  $\alpha_k = -1/2$  ( $\alpha = 1/2$ ). However, the short distances in the BA model and the exponential decay indicate a finite-size effect [16].

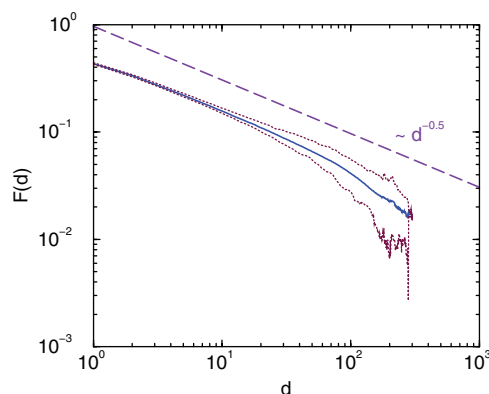


Fig. 3: (Colour on-line) Degree fluctuation function of the  $z = 3$  Cayley tree at percolation transition. The fluctuation function,  $F(d)$ , is plotted against the length of the shortest paths  $d$ . The dotted maroon lines represent the quantiles enclosing 90% of the 100 configurations (each). The dashed straight line is a guide to the eye and corresponds to the exponent  $\alpha_k = -1/2$ .

*Cayley tree.* Since many complex networks are small world, their diameter is rather small and therefore the largest distance  $d$  for which the fluctuation function can be calculated is also small (see figs. 2a, b). To overcome this issue we first study a tree structure, the Cayley tree at the percolation transition. The fractal nature of this system allows us to analyze the fluctuation function at longer ranges of  $d$ . The Cayley tree [17,18] is built by starting from a central node and attaching  $z$  new nodes to it. In the next generation  $z - 1$  additional nodes are linked to each of the new nodes of the previous generation. All nodes except the ending ones have degree  $z$ . In percolation, starting from the complete Cayley tree, elements of the tree are randomly removed. In this case, the percolation transition is at  $p_c = \frac{1}{z-1}$  [18] and the topological dimension of the giant component is  $d_f = 2$  [17].

Figure 3 depicts the fluctuation functions  $F(d)$  for the Cayley tree with  $z = 3$  in generation  $n = 150$  at the percolation transition (together with the quantiles enclosing 90% of the configurations). In this case all node degrees are within the range  $1 \leq k \leq 3$ . For  $2 < d < 80$  the fluctuation function follows a power law according to eq. (1) with  $\alpha_k \simeq -1/2$  ( $\alpha \simeq 1/2$ ), indicating uncorrelated degrees of the nodes along the paths. The deviations from the power law at large distances are due to the finite size of the networks. Since the removal of elements of the Cayley tree happens randomly and in particular independent of each other, fig. 3 is in agreement with what we expect ( $\alpha_k \simeq -1/2$  corresponds to uncorrelated degrees), supporting the proposed technique.

*Fractal network model.* We now use the fractal network model introduced by Song, Havlin, and Makse [5] in which the diameter grows with the network size as  $N^{1/d_f}$ . It has been shown that anticorrelations between node degrees are a determinant factor for the fractality of a network [5,19–22].

The fractal network is built iteratively (an illustration can be found in ref. [22]). It starts in generation  $n=0$  with 2 nodes connected by 1 link. In generation  $n+1$ ,  $m$  new nodes are attached to the endpoints of each link of the previous generation. i) With probability  $1-e$  the corresponding link of generation  $n$  is removed and  $x \leq m$  new links are added between the new nodes. ii) With probability  $e$  the corresponding link remains and  $x-1$  new links connect the new nodes. We use  $m=2$ ,  $x=2$ , and  $n=3, 4, 5$ . In the case of  $e=0$ , in the first generation the network represents a hexagon consisting of 6 nodes and 6 links. In the second generation, each link of the hexagon is replaced by another hexagon, and so on. The larger  $e$ , the more short-cuts are produced and the more small-world-like the generated network is. Thus, according to the parameter  $e$ , the network is fractal ( $e=0$ ) comprising large diameter or non-fractal ( $e=1$ ) being small world. On the other hand, although  $m$  and  $x$  do not alter whether the network is fractal or not, they are relevant for the number of nodes in the network, for node degrees, and for the number of possible paths between pairs of nodes [5]. For example, a large value of  $m$  generates a faster increase in the number of nodes, and a larger  $x$  generates more cycles and paths between any pair of nodes. All three parameters,  $m, x, e$  affect the fractal dimension,  $d_f$ , of the network which is given by [5,22]

$$d_f = \frac{\ln(2m+x)}{\ln(3-2e)}. \quad (5)$$

The expression diverges when  $e=1$  for a pure small-world network. For  $m=2$ ,  $x=2$  it is  $d_f = \frac{\ln(6)}{\ln(3-2e)}$ . The degree distribution is given by  $p(k) \sim k^{-(1+\frac{\ln(2m+x)}{\ln m})}$  [5].

To analyze this model we generate many configurations and apply the fluctuation analysis. Figure 4 shows the degree fluctuation functions for the model in generation  $n=4$  and different values of  $e$ . For  $e=0$  (fractal) the fluctuation function decreases as  $F(d) \sim d^{-1}$ , thus  $\alpha_k = -1$ , whereas  $F(d)$  exhibits some structure which is due to the deterministic character of the model when  $e=0$ , *i.e.* for certain distances the sequences of degrees are identical leading to vanishing standard deviation among the paths. In the case of  $e=0.06$ , the fluctuation function also decreases as a power law but with an exponent  $\alpha_k \approx -0.7$ . Due to finite size effects,  $F(d)$  exhibits deviations from a power law for  $d > 60$ . For  $e=0.24$ , fig. 4c, although the network diameter decreases compared to smaller values of  $e$ , we still find a power law regime over more than 1 decade. The inset of fig. 4c shows the fluctuation functions for  $n=3$  and  $n=5$ . These power law decays support the conjecture of long-range correlations. Since  $\alpha = \alpha_k + 1 < 1/2$ , the degrees are anticorrelated, consistent with previous findings. The case  $e=1$ , where the networks is small world, is depicted in fig. 4d. The diameter is much smaller and the decay is close to exponential.

Next, to obtain the exponents  $\alpha_k$  we apply least-squares fits to  $F(d)$ . In fig. 5 the exponents  $\alpha = \alpha_k + 1$  are

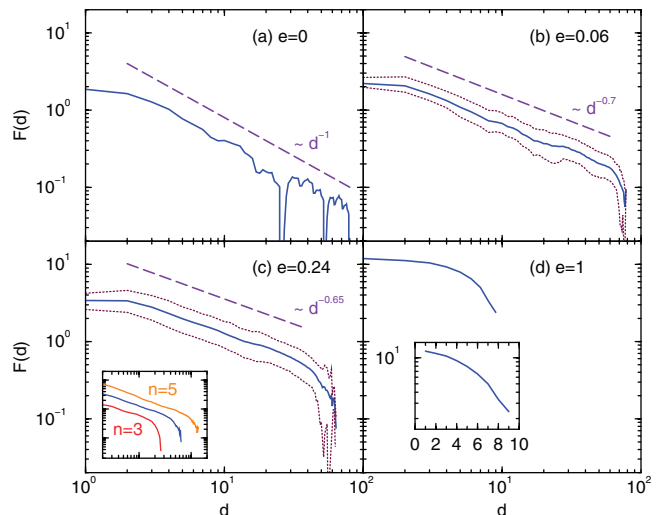


Fig. 4: (Colour on-line) Degree fluctuation functions for the fractal model in the fourth generation ( $n=4$ ). The fluctuation functions,  $F(d)$ , are plotted against the length of the shortest paths  $d$ , for (a)  $e=0$ , (b)  $e=0.06$ , (c)  $e=0.24$ , and (d)  $e=1$ . The dotted maroon lines in (b) and (d) represent the quantiles enclosing 90% of the 250 configurations (each). The dashed straight lines are guides to the eye and correspond to the exponents (a)  $\alpha_k = -1$ , (b)  $\alpha_k = -0.7$ , and (c)  $\alpha_k = -0.65$ . The cases  $e=0$  and  $e=1$  are deterministic and accordingly there are no uncertainty levels. Panel (c) contains an inset with the  $F(d)$  for the model with  $e=0.24$  in third ( $n=3$ ) and fifth ( $n=5$ , 25 configurations) generation. The inset in panel (d) is the same as the major panel but in linear-log representation.

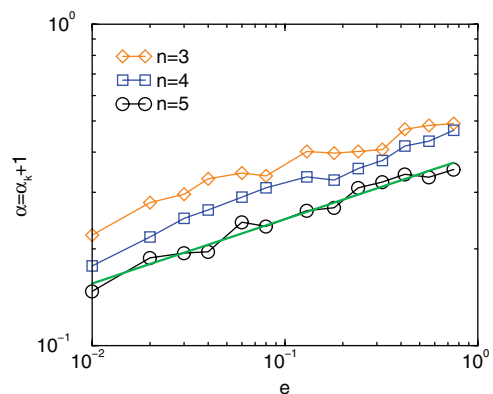


Fig. 5: (Colour on-line) Exponents of the fractal network model. The exponents  $\alpha = \alpha_k + 1$  are plotted as a function of the model parameter  $e$ . The  $\alpha_k$ -values were obtained from least-squares fits to the fluctuation functions as exemplified in fig. 4. We use the model in third, fourth, and fifth generation ( $n=3$ ,  $n=4$ : 250 configurations;  $n=5$ : 25 configurations). The green straight solid line represents a power law fit to the exponents for  $n=5$  leading to  $\alpha_k + 1 = \alpha \sim e^\epsilon$  with  $\epsilon \approx 0.2$ .

plotted against the model parameter  $e$  for the networks in generations  $n=3, 4, 5$ . We find that the curves of  $\alpha$  vs.  $e$  are parallel for all three values of  $n$ . However, the actual value of  $\alpha_k$  systematically decreases with the generation  $n$  due to finite-size effects. Although the range of  $\alpha$  is rather

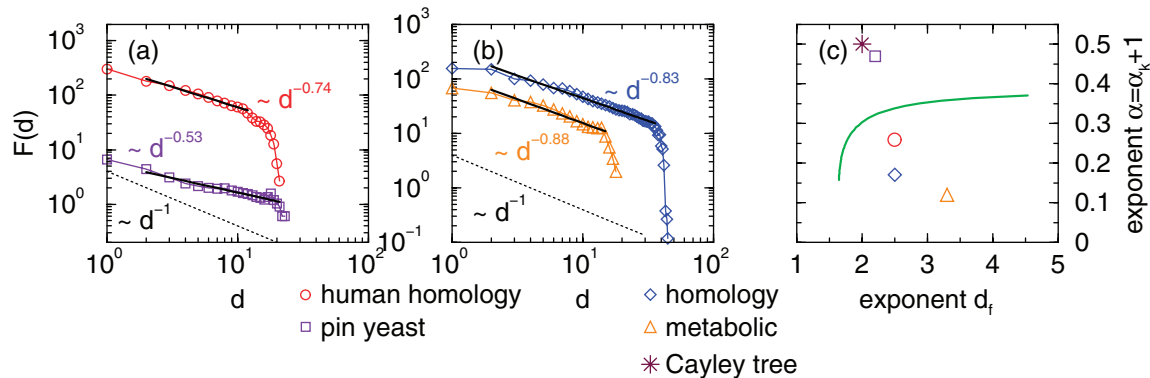


Fig. 6: (Colour on-line) Degree fluctuation functions for real-world networks and comparison of the fluctuation exponents with fractal dimension  $d_f$ . The fluctuation functions,  $F(d)$ , are plotted against the length of the shortest paths  $d$ , for (a) the human homology network (red circles), the pin yeast network (indigo squares), and (b) the homology network (blue diamonds), as well as the metabolic network (orange triangles). The black solid straight lines are regressions providing the exponents (a)  $\alpha_k \simeq -0.74$  (human homology network,  $d_f \simeq 2.5$ ),  $\alpha_k \simeq -0.53$  (pin yeast network,  $d_f \simeq 2.2$ ), and (b)  $\alpha_k \simeq -0.83$  (homology network,  $d_f \simeq 2.5$ ), as well as  $\alpha_k \simeq -0.88$  (metabolic network,  $d_f \simeq 3.3$ ). The black dotted straight lines in the bottom of ((a),(b)) correspond to the exponent  $\alpha_k = -1$ . (c) Fluctuation exponent  $\alpha = \alpha_k + 1$  vs. fractal dimension  $d_f$ . The solid line corresponds to the fit of  $\alpha(e)$  from fig. 5, and the asterisk is the corresponding value for the Cayley tree. The values of the real-world networks are given by the corresponding symbols.

small, we exclude a logarithmic dependence of  $\alpha$  on  $e$  since for  $e = 0$  we find  $\alpha = 0$ . Applying the regression  $\alpha \sim e^\epsilon$  to the  $n = 5$  exponents we find  $\epsilon \approx 0.2$ .

*Real-world networks.* The fluctuation analysis serves as a tool to unravel the long-range degree correlations present in real-world networks. In this section we study the long-range degree correlations in 4 biological networks, i) the Protein Interaction Network of Yeast [23], with 777 nodes and 1797 links in which two proteins of the Yeast cell are connected if they interact chemically with each other, ii) the Metabolic Network of *E. coli* [24], with 2859 nodes and 6890 links, in which metabolites within the *E. coli* cell interact biochemically with each other, iii) the Human Homology Network [25], with 21710 nodes and 1289345 links, where proteins of the human cell are connected through a link if they are biologically homologous (their sequence of amino-acids present an E-value smaller than  $10^{-30}$ ) and iv) the Homology Network of 251 Prokaryotic Genomes [26], with 30727 nodes and 1206654 links, in which proteins of different organism are connected through a link if they are biologically homologous. These 4 networks have been found to exhibit fractality [5,6,19,20].

Figures 6a, b show the fluctuation functions obtained for these real-world networks. The curves exhibit power law decays over a wide range of  $d$ . For large scales deviations are found that are due to the finite size of the networks, similarly to what is seen for the fractal network model. We obtain the exponents  $\alpha_k \simeq -0.53$  (pin yeast),  $\alpha_k \simeq -0.74$  (human homology),  $\alpha_k \simeq -0.83$  (homology), and  $\alpha_k \simeq -0.88$  (metabolic). In fig. 6c the corresponding  $\alpha = \alpha_k + 1$  are compared with the fractal dimension values that have been found before [5,6,19,20]. The panel also contains the results for the Cayley tree and the fit for

the fractal model ( $n = 5$ ) from fig. 5 when the values  $d_f$  are calculated according to eq. (5) and with the model parameters ( $m = 2$ ,  $x = 2$ , variable  $e$ ).

The idea of fig. 6c is to compare the fractal dimension with the fluctuation exponent. Although our results for the real-world networks are scattered in fig. 6c, they display a decrease in  $\alpha$  as  $d_f$  increases. The Cayley tree seems to follow the same trend. In contrast, the simulations in the fractal model reflect the opposite. This suggests that  $d_f$  might not be the only quantity related to degree anticorrelations and that the fluctuation exponent provides complementary information. Further studies, which are beyond the scope of this work, are necessary to completely determine the variables affecting the value of  $\alpha$ .

**Discussion and outlook.** – In summary, a method for the characterization of spatial degree correlations in complex networks is suggested. The technique is based on fluctuation analysis in analogy to methods used in times series analysis. The fluctuation analysis is applied to the degrees of i) the BA model, ii) the Cayley tree at percolation, iii) the fractal network model, and iv) examples of real-world networks. It is found that fluctuation functions of the BA model decay exponentially. In contrast, the degree correlations in the fractal network model decay as a power law and according to the obtained exponents the degrees comprise long-range anticorrelations. Further studies are needed to obtain a better understanding of a possible connection between power law anticorrelations and fractality of complex networks.

Such long-range anticorrelations may have structural implications regarding the stability of networks with respect to random removals [27]. Long-range correlations

could also have an influence on correlations between the degree and the betweenness centrality of nodes [28]. Possible applications include disease spreading, see, *e.g.*, [29] and references therein, where it is important whether large-degree nodes tend to be linked to other large-degree nodes or if such hubs are separated by small-degree nodes, and how correlations at larger distances influence the spreading. Other applications could be climate networks [30–32].

Nevertheless, further research is needed to evaluate the proposed fluctuation analysis and the possible dependence of the fluctuation exponents on the system size. In addition, an analytical description of the models is aimed in order to gain a better comprehension of long-range correlations in complex networks. Furthermore, it would be interesting to vary the model parameters  $m$  and  $x$  and to study other fractal networks, as well as more real-world networks.

Fractality and the small-world property, two seemingly contradicting properties are known to coexist in real-world networks [21]. Typically real-world networks are found to be fractal up to a certain length scale until the small-world property kicks in at global scale. Therefore, the method presented in this paper may also be applied to networks that are small world and is not limited to fractal networks.

Finally, we would like to point out that our approach can also be extended to study other spatial correlations. These can be i) various network properties, as long as they can be attributed to the nodes or edges, such as clustering, betweenness centrality, and many others, or ii) additional information available in the form of characteristic values assigned to the nodes (time of addition of the node to the network, activity of the node, etc.), or to the links (weight, activity, stability, etc.). In addition, one could think about including dynamics and analyze spatio-temporal correlations.

\*\*\*

We wish to thank the Baltic Sea Region Programme (2007-2013) for supporting the BaltCICA project. We thank J. W. KANTELHARDT for helpful insight on our analysis.

## REFERENCES

- [1] NEWMAN M. E. J., *Phys. Rev. Lett.*, **89** (2002) 208701.
- [2] NEWMAN M. E. J., *Phys. Rev. E*, **67** (2003) 026126.
- [3] PASTOR-SATORRAS R., VÁZQUEZ A. and VESPIGNANI A., *Phys. Rev. Lett.*, **87** (2001) 258701.
- [4] MASLOV S. and SNEPPEN K., *Science*, **296** (2002) 910.
- [5] SONG C. M., HAVLIN S. and MAKSE H. A., *Nat. Phys.*, **2** (2006) 275.
- [6] GALLOS L. K., SONG C. and MAKSE H. A., *Phys. Rev. Lett.*, **100** (2008) 248701.
- [7] PENG C.-K., BULDYREV S. V., GOLDBERGER A. L., HAVLIN S., SCIORTINO F., SIMONS M. and STANLEY H. E., *Nature*, **356** (1992) 168.
- [8] KOSCIELNY-BUNDE E., BUNDE A., HAVLIN S., ROMAN H. E., GOLDBREICH Y. and SCHELLNHUBER H.-J., *Phys. Rev. Lett.*, **81** (1998) 729.
- [9] KOUTSOYIANNIS D., *J. Hydrol.*, **324** (2006) 239.
- [10] KANTELHARDT J. W., *Fractal and multifractal time series*, in *Encyclopedia of Complexity and Systems Science*, edited by MEYERS R. A. (Springer) 2009, pp. 3754–3779.
- [11] KANTELHARDT J. W., KOSCIELNY-BUNDE E., REGO H. H. A., HAVLIN S. and BUNDE A., *Phys. A*, **295** (2001) 441.
- [12] PENG C.-K., MIETUS J., HAUSDORFF J. M., HAVLIN S., STANLEY H. E. and GOLDBERGER A. L., *Phys. Rev. Lett.*, **70** (1993) 1343.
- [13] BAHAR S., KANTELHARDT J. W., NEIMAN A., REGO H. H. A., RUSSELL D. F., WILKENS L., BUNDE A. and MOSS F., *EPL*, **56** (2001) 454.
- [14] MA Q. D. Y., BARTSCH R. P., BERNAOLA-GALVÁN P., YONEYAMA M. and IVANOV P. C., arXiv:1001.3641v1 [physics.data-an] (2010).
- [15] BARABÁSI A.-L. and ALBERT R., *Science*, **286** (1999) 509.
- [16] LENNARTZ S. and BUNDE A., *Phys. Rev. E*, **79** (2009) 066101.
- [17] HAVLIN S. and NOSSAL R., *J. Phys. A: Math. Gen.*, **17** (1984) L427.
- [18] BEN-AVRAHAM D. and HAVLIN S., *Diffusion and Reactions in Fractals and Disordered Systems* (Cambridge University Press, Cambridge) 2004.
- [19] SONG C. M., HAVLIN S. and MAKSE H. A., *Nature*, **433** (2005) 392.
- [20] GALLOS L. K., SONG C., HAVLIN S. and MAKSE H. A., *Proc. Natl. Acad. Sci. U.S.A.*, **104** (2007) 7746.
- [21] ROZENFELD H. D., SONG C. and MAKSE H. A., *Phys. Rev. Lett.*, **104** (2010).
- [22] ROZENFELD H. D. and MAKSE H. A., *Chem. Eng. Sci.*, **64** (2009) 4572.
- [23] HAN J.-D. J., BERTIN N., HAO T., GOLDBERG D. S., BERRIZ G. F., ZHANG L. V., DUPUY D., WALHOUT A. J. M., CUSICK M. E., P. R. F. and VIDAL M., *Nature*, **430** (2004) 88.
- [24] ALMAAS E., KOVACS B., VICSEK T., OLTVAI Z. N. and BARABASI A.-L., *Nature*, **427** (2004) 839.
- [25] ARNOLD R., RATTEI T., TISCHLER P., TRUONG M.-D., STUMPFLER V. and MEWES W., *Bioinformatics*, **21** (2005) 42.
- [26] MEDINI D., COVACCI A. and DONATI C., *PLoS Comput. Biol.*, **2** (2006) e173.
- [27] COHEN R., EREZ K., BEN AVRAHAM D. and HAVLIN S., *Phys. Rev. Lett.*, **85** (2000) 4626.
- [28] KITSACK M., HAVLIN S., PAUL G., RICCABONI M., PAMMOLLI F. and STANLEY H. E., *Phys. Rev. E*, **75** (2007) 056115.
- [29] KITSACK M., GALLOS L. K., HAVLIN S., LILJEROS F., MUCHNIK L., STANLEY H. E. and MAKSE H. A., arXiv:1001.5285v1 [physics.soc-ph] (2010).
- [30] YAMASAKI K., GOZOLCHIANI A. and HAVLIN S., *Phys. Rev. Lett.*, **100** (2008) 228501.
- [31] TSONIS A. A. and SWANSON K. L., *Phys. Rev. Lett.*, **100** (2008) 228502.
- [32] DONGES J. F., ZOU Y., MARWAN N. and KURTHS J., *EPL*, **87** (2009) 48007.